July 2001

ELSEVIER

Materials Letters 49 (2001) 294–298

MATERIALS LETTERS

www.elsevier.com/locate/matlet

Textured strontium ferrite thin films grown by PLD

T. García [a], E. de Posada [a], L. Ponce [a], J.L. Sánchez [a], S. Díaz [a], E. Pedrero [a], F. Fernández [a], P. Bartolo-Pérez [b,*], J.L. Peña [b,c], R. Diamant [d], J.A.M. Pereira [e]

[a] *IMRE-Physics Faculty, Havana University, Havana, Cuba*
[b] *CINVESTAV-IPN, Mérida, Applied Physics Department, A.P. 73 Cordemex, 97310 Mérida, Yuc., Mexico*
[c] *CICATA-IPN, Altamira, Tamps, Mexico*
[d] *UAM-Unidad Izpalapa, D.F., Mexico*
[e] *Pontifícia Universidade Católica do Rio de Janeiro, Rio de Janeiro, Brazil*

Received 20 October 2000; received in revised form 24 October 2000; accepted 24 October 2000

Abstract

Textured strontium ferrite thin films has been grown at room temperature using a Nd:YAG laser. The spectroscopic study of the produced plasma revealed that the expansion velocities of the species are of the order of 10^6 cm/s, which could explain the obtained texture. The stoichiometric analysis shows a small oxygen reduction in the films due to the absence of a gas background during the growing process. The influence of the target quality on the droplet presence at the thin films has been investigated.

PACS: 81.15.Fg; 81.70.Jb; 82.80.Pv; 87.64.Dz; 87.64.Ee
Keywords: Strontium ferrite; Ferromagnetic oxide ($MFe_{12}O_{19}$); Textured thin films; Laser ablation; XPS; AES

1. Introduction

The usual high substrate temperatures needed for the growth of textured or epitaxial thin films represent, often, a technologic problem. Laser ablation is a technique that can avoid this problem in some materials. Here, we present interesting results on the growing of strontium ferrite textured thin films.

The huge expansion in the 1990s of the applications of the recording magnetic media has caused an increase of the interest on the different methods for growing of polycrystalline thin films based on hexagonal ferrites, where M Ferrites ($MFe_{12}O_{19}$, where M = Ba, Sr, Pb) are among the most promising materials [1]. Techniques such as radio frequency (rf) sputtering [2–4], metal–organic chemical vapor deposition (MOCVD) [5], metal–organic decomposition (MOD) [6], sol–gel [7] and laser ablation [8,9] have been used for the growing of these materials.

Laser ablation shows some advantages especially for the growing of multi-component materials in both the final stoichiometry and the low substrate temperature needed to obtain crystallinity. It had been reported that without the use of substrate heating, thin films of barium M ferrites grown by rf sputtering only could be amorphous [10].

* Corresponding author. Tel.: +52-9-9812-929; fax: +52-9-9812-917.
E-mail address: pascual@mda.cinvestav.mx (P. Bartolo-Pérez).

00167-577X/01/$ - see front matter
PII: S0167-577X(00)00387-6

2. Experimental

The growth process was carried out in a typical laser ablation setup, an HV chamber under a pressure of 10^{-3} Pa within which was placed the rotating target holder for the $SrFe_{12}O_{19}$ sintered ceramic. Each evaporation consisted of 2000 pulses from a Q-switched Nd:YAG laser at 5 Hz and under an angle of incidence on the target of 45°. The energy of the laser pulse was 250 mJ, a duration of 20 ns and the power density was about 10^9 W/cm^2. The ablated material was deposited on a Si (100) substrate placed at 25 mm from the target and at room temperature.

The surface morphology of the films was studied using scanning electron microscopy (SEM). Jeol JSM-35C equipment operated at $E = 25$ keV was used to take the SEM micrograph. The chemical composition measurements were carried out using an Auger electron spectroscopy (AES), X-ray photoelectron spectroscopy (XPS) and Rutherford backscattering spectroscopy (RBS). AES and XPS analyses were performed in a Perkin-Elmer PHI 560/ESCA-SAM system, equipped with a double-pass cylindrical mirror analyzer, with a base pressure of 1×10^{-9} Torr. For the XPS analysis, samples were excited with 1486.6 eV energy $Al_{K\alpha}$ X-rays. The spectrometer was calibrated using the Cu $2p_{3/2}$ (932.4 eV) and Cu $3p_{3/2}$ (74.9 eV) lines. Binding energy calibration was based on C 1s at 284.6 eV. RBS analyses were performed using $^4He^+$ ion beam with 2.0 MeV from a Van de Graff accelerator, with a Si(Li) detector and a resolution of 17 keV. X-ray diffraction (XRD) analysis in the grazing incidence geometry were done under CuK_α radiation at 40 kV with 35 mA, using a D5000 Siemens X-ray diffractometer with monochromatic radiation ($\lambda = 1.5418$ Å). The spectroscopic studies of the plasma were carried out using a setup described in a previous paper [11].

3. Results and discussion

Fig. 1 shows the SEM micrograph of the target surface both before and after a repetitive action of the laser pulses. In the first case (a), the grains formed during the ceramic sintering can be seen and for the second (b), a melting in the target surface reveals a large thermal component during the ablation process. Also, it shows a comparison between the surface qualities of the films obtained from ablation of a target surface similar to ones shown in Fig. 1(a) and (b). In the first case (c), there is a large density of droplets, mainly spherical particles, which have suffered a melting process and because the

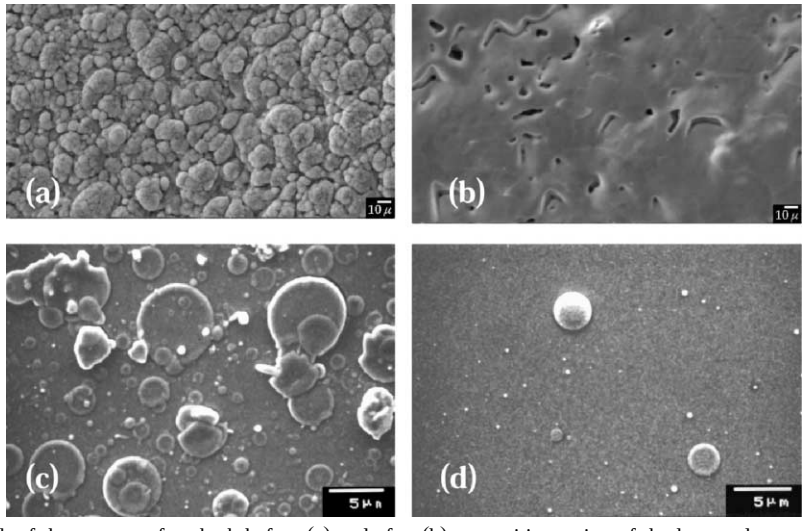

Fig. 1. SEM micrograph of the target surface both before (a) and after (b) a repetitive action of the laser pulses, and SEM micrograph (c) and (d) of the surfaces of the films obtained under the ablation of the previous target surfaces, respectively.

droplets temperatures are higher than the fusion temperature of the target material they acquire this shape [12–14]. The other particles with irregular shape suggest the presence of an exfoliational mechanism during the process [15]. On the other hand (d), the films obtained after repetitive incidence of the laser pulses show a marked reduction in the droplets density. Next, only the films obtained under the last conditions will be taken.

Although the results of the XPS and RBS spectra show that the concentration of the elements Fe and Sr were the same in the films as in the target, it was not the same for the concentration of oxygen. In Fig. 2, we present the target and film normalized derivative Auger spectra for O and Fe transitions. In the film, there is a small increase in the peak to peak intensity in the Fe peaks, which is proportional to the concentration of this element in the film, suggesting a loss of oxygen during the process. This can be corroborated if we look at the XPS spectra of the Fe peaks $2p_{1/2}$ and $2p_{3/2}$ showed in the Fig. 3. The spectra, belonging to the target, shows the typical shape of the O–Fe bound with the maximum of the Fe $2p_{3/2}$ peak located at 710 eV of the bounding energy. In the case of the film, for the same peak, there is an appearance of a shoulder suggesting also the presence of Fe metallic, suggesting the possibility of oxygen vacancies, although small in quantity. This is an expected result if we take into account that

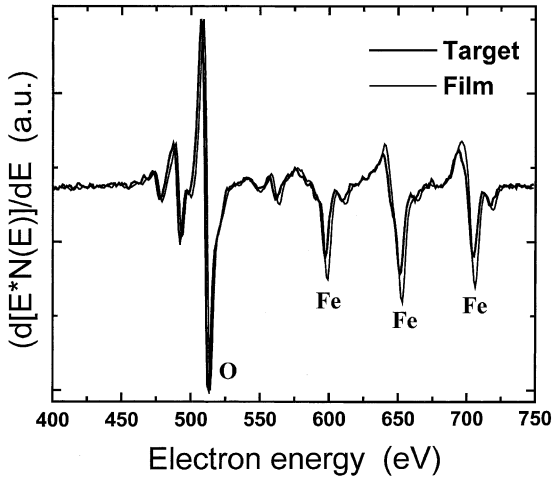

Fig. 2. AES spectra of both (a) the $SrFe_{12}O_{19}$ target and (b) the film.

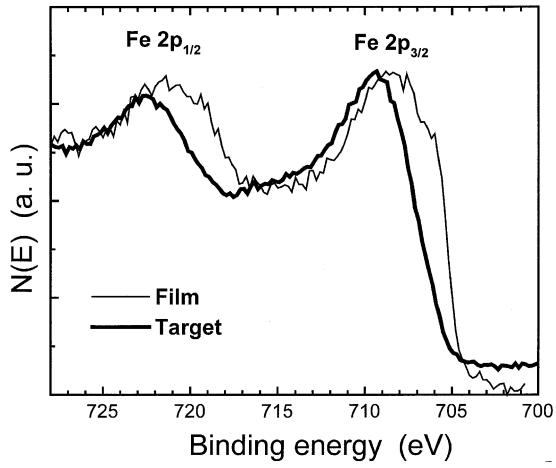

Fig. 3. XPS spectra Fe 2p of both the $SrFe_{12}O_{19}$ target and the film.

oxygen is the lighter element of the species within the plume, so it can acquire higher velocities, suffer more dispersive collisions and also reach the substrate first. This, combined with its high vapor pressure, reduces its probability to condensate on the growing film. The calculus of relative atomic concentration using XPS and RBS analyses shows that the films stoichiometry is around $SrFe_{12}O_{15}$.

The typical XRD spectra for both (a) the target and (b) the film are shown in the Fig. 4. The observation of the spectra corresponding to the film suggests a textured grown. We assume that this behavior, mainly, is due to the high kinetic energies and the high deposition rate of the plume species, which cause an increase on the surface temperature of the film that is growing. The monocrystallinity of the selected substrate could also help on this result.

In order to calculate the species velocities within the plume, we performed the time of flight (TOF) analysis of the different species using optical emission spectroscopy. For this task, we selected the atomic lines of SrI ($\lambda = 4607.33$ Å), FeI ($\lambda = 3581.2$ Å), OI ($\lambda = 7774$ Å), simple ions SrII ($\lambda = 4077.71$ Å) and FeII ($\lambda = 6456.38$ Å). All the measurements were performed at different points between the target and the substrate. Fig. 5 shows the result of the TOF analysis for FeI. The mean velocities of the plume species were calculated from the maximum of the different TOF curves. The results of this calculus are

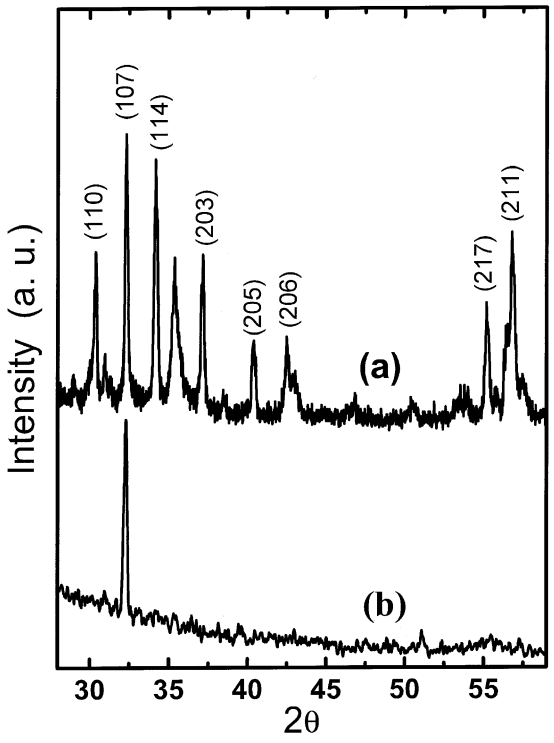

Fig. 4. XRD spectra of both (a) the $SrFe_{12}O_{19}$ target and (b) the film.

shown in Fig. 6. Although there are some differences, all the species velocities were of the order of 10^6 cm/s. The higher velocities were detected for ionic species, suggesting their faster arrival to the substrate.

Generally, it is required to heat the substrate to obtain crystallinity in the film. In our case, this

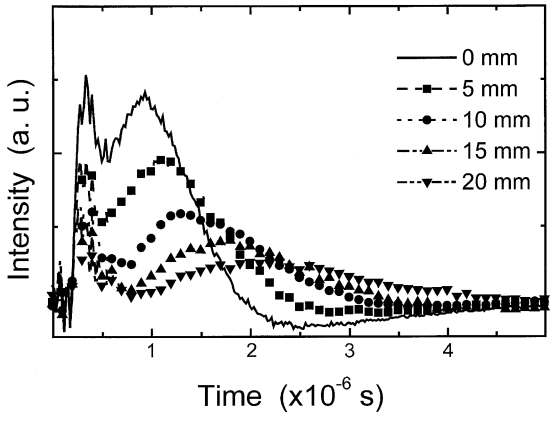

Fig. 5. Time of flight spectra of Fe atoms.

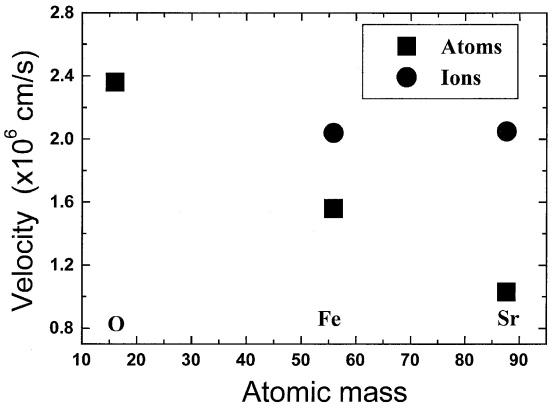

Fig. 6. Calculated mean velocities of the species.

temperature is obtained from the high velocity species due to the energy transference during the collision with the substrate. For plasmas produced by lasers with nanosecond pulse length, the heating is produced only in the first few microns of the surface and remains for some microseconds. The maximum temperature reached is linear to the mean kinetic energy of the incident particles [16]. The collision of the ions, with energies over 100 eV, on the substrate cause the formation of a thin layer (similar to tens of Ångström) of individual vacancies, which start a diffusion throughout the substrate and recombine again within a time about 10^{-8} s, without significantly affecting the crystallinity [17]. These vacancies are of extreme importance for the adhesion of the atoms to the film that is growing. In this case, it should be also taken into account the influence of the used short target–substrate distance on the temperature, as it has been reported the increase of the surface temperature is proportional to $1/d^2$, where d is the target–substrate distance [16].

The analysis of the RBS spectra gave a film thickness of 520 nm, giving a growth rate of 2.6 Å/pulse. Working with the TOF at the position of the substrate, we have obtained an evaporation rate of 4.8×10^5 Å/s, a high value compared with the other deposition techniques. The high evaporation rate causes the condensation heat, which is proportional to the quantity of material deposited, to dissipate to the film followed by a thermal diffusion. For higher deposition rate, the thermal diffusion process can suffer a "jam" causing all the heat to be deliv-

ered to a very thin layer of the film acting as an effective heat source.

4. Conclusions

We have demonstrated the possibility of growing strontium ferrite thin films using laser ablation at room temperature. The XRD spectra show a textured growth caused principally by the high kinetic energy of the species, the short target–substrate distance and the high evaporation rate ($\sim 10^5$ Å/s). Although the concentration of Fe and Sr remained the same as in the target, there was a small reduction of oxygen due to the absence of an oxygen background. The relation between droplets and the smoothness of the target surface has been demonstrated.

Acknowledgements

The authors would like to thank E. Haro-Poniatowski, W. Cauich, V. Rejón and M. Herrera for technical support. We also thank E.F. Da Silveira and the CLAF for their help on the analysis of the RBS.

References

[1] D. Speliotis, M. Dugas, J. Humenansky, K.L. Babcok, K. Peter, J. Appl. Phys. 81 (1997) 3830.
[2] B.R. Acharya, S. Prasad, N. Venkataramani, E.N. Abarra, T. Suzuki, IEEE Trans. Magn. 33 (1997) 3640.
[3] A. Morisako, M. Matsumoto, S. Takei, T. Yamazaki, IEEE Trans. Magn. 33 (1997) 3100.
[4] B.Y. Wong, X. Sui, D.E. Laughlin, M.H. Kryder, J. Appl. Phys. 75 (1994) 5966.
[5] E.J. Donahue, D.M. Schleich, J. Appl. Phys. 71 (1992) 6013.
[6] S. Díaz, J.L. Sánchez, B.E. Watts, F. Leccabue, R. Panizzieri, J. Magn. Magn. Mater. 151 (1995) 173.
[7] C. Surig, K.A. Hempel, D. Bonnenberg, Appl. Phys. Lett. 63 (1993) 2836.
[8] P.C. Dorsey, S.B. Qadri, K.S. Growoski, D.L. Kenies, P. Lubitz, D.B. Chrisey, J.S. Horwitz, Appl. Phys. Lett. 70 (1997) 1173.
[9] R. Nawathey-Dikshit, S.R. Shinde, S.B. Ogale, S.D. Kulkarni, S.R. Sainkar, S.K. Date, Appl. Phys. Lett. 68 (1996) 3491.
[10] B.Y. Wong, X. Sui, D.E. Laughlin, M.H. Kryder, J. Appl. Phys. 75 (1994) 5966.
[11] R. Diamant, E. Jimenez, E. Haro-Poniatowski, L. Ponce, M. Fernandez-Guasti, J.C. Alonso, Diamond Relat. Mater. 8 (1999) 1277.
[12] W.K.A. Kumuduni, Y. Nakata, Y. Sasaki, T. Okada, M. Maeda, T. Kisu, M. Takeo, K. Enpuku, J. Appl. Phys. 77 (1995) 5961.
[13] D.B. Geohegan, Appl. Phys. Lett. 62 (1993) 1463.
[14] H. Wakata, E. Tasev, M. Tuda, K. Ono, K. Haruta, Y. Ueda, Appl. Surf. Sci. 79–80 (1994) 152.
[15] R. Kelly, J.J. Cuomo, P.A. Leary, J.E. Rothenberg, B.E. Braren, C.F. Aliotta, Nucl. Instrum. Methods Phys. Res. B 9 (1985) 329.
[16] X. Xu, J. Appl. Phys. 77 (1995) 6715.
[17] S. Metev, in: B.C. Douglas, K.H. Graham (Eds.), Pulsed Laser Deposition of Thin Films, Wiley, New York, 1994, 255.